

PAPER • OPEN ACCESS

Etched Silicon Planar CRL Optics for the High-Energy X-ray Diffraction Beamlines 11-ID-B and 11-ID-C at the APS

To cite this article: Uta Ruett *et al* 2022 *J. Phys.: Conf. Ser.* **2380** 012060

View the [article online](#) for updates and enhancements.

You may also like

- [DETAILED CHEMICAL ABUNDANCES OF FOUR STARS IN THE UNUSUAL GLOBULAR CLUSTER PALOMAR 1](#)
Charli M. Sakari, Kim A. Venn, Mike Irwin et al.
- [High energy surface x-ray diffraction applied to model catalyst surfaces at work](#)
Uta Hejral, Mikhail Shipilin, Johan Gustafson et al.
- [High energy X-ray nanofocusing by silicon planar lenses](#)
A Snigirev, I Snigireva, M Grigoriev et al.

ECS Toyota Young Investigator Fellowship



For young professionals and scholars pursuing research in batteries, fuel cells and hydrogen, and future sustainable technologies.

At least one \$50,000 fellowship is available annually.
More than \$1.4 million awarded since 2015!



Application deadline: January 31, 2023

Learn more. Apply today!

Etched Silicon Planar CRL Optics for the High-Energy X-ray Diffraction Beamlines 11-ID-B and 11-ID-C at the APS

Uta Ruett¹, Lisa Gades¹, Olaf Borkiewicz¹, Orlando Quaranta¹, Kevin Beyer¹,
Guy Jennings¹, C. Suzanne Miller², and Antonino Miceli¹

¹ X-ray Science Division, Argonne National Laboratory, Lemont, IL 60439, U.S.A

² Nanoscience & Technology, Argonne National Laboratory, Lemont, IL 60439, U.S.A

uruett@anl.gov

Abstract. The focusing of high-energy X-rays is most commonly achieved by commercially available compound refractive lenses (CRL), which are added together in larger structures. There is a need for high-energy X-ray beamlines to enable focusing in only one dimension down to a few micrometers to study layered materials and thin films. High-energy X-rays above 50 keV require often 100 lenses or more, therefore it is more efficient to etch the complete arrays of lenses into a monolithic substrate like a silicon wafer. Custom lens arrays were fabricated for the high-energy x-ray beamlines 11-ID-B, and 11-ID-C at the Argonne National Laboratory. The fabrication required tuning parameters of the Bosch process to optimize the etching of deep vertical sidewalls at a reasonable speed without overheating. The beamline 11-ID-B is equipped with lens arrays of 85-110 lenses for 59 keV and 190-250 lenses for 87 keV photon energy, focusing the beam vertically below 5.0 μm at the sample positions between 1600 mm to 2100 mm. 11-ID-C has received arrays of 435 lenses that focus 106 keV X-rays to a vertical height of 2.0 μm at the sample position. In both cases, the flux density gain in the focal spot is larger than a factor of 20, relative to using slits to cut the beam size. The lens setup is permanently installed and can be moved in and out of the beam during the experiment without further alignment. The lenses have enabled *operando* diffraction studies on interfaces in batteries and the development of pair distribution function (PDF) analysis using grazing incidence geometry.

1. Motivation

The focusing of high-energy X-rays with photon energies larger than about 50 keV is most commonly achieved with compound refractive lenses (CRLs) made of aluminum [1,2] using dies to press individual lenses. They are formed either as 1-dimensional (line focusing) or 2-dimensional parabolic shapes (point focusing) [3]. Saw-tooth lenses made of silicon [4,5] or planar parabolic lenses etched in silicon as developed by Aristov et al. [6] and explored in great detail by others [7, 8,9] are great choices for compact 1D lens structures for line foci. Another process is LIGA (lithography, electroplating, and molding) using nickel for high-energy x-rays [10]. While the individual aluminum lenses are commercially available, the silicon parabolic lenses are fabricated for research projects. The aluminum lenses can be purchased as 2D lenses for focusing with a radius down to 50 μm , but the 1D-lenses are more difficult to produce and therefore only offered with a larger radius of 100 μm [3]. The number N of bi-concave lenses required for a focal length F and photon energy E or wavelength λ depends on the radius R of the lenses with parabolic shape, Figure 1, and the refractive index δ of the chosen material:

$$N = \frac{R}{2 \delta F} \quad \text{with} \quad \delta = \frac{N_A r_0 \lambda^2 \rho Z}{2 \pi A} \quad (1)$$

for high photon energies beyond absorption edges, where N_A is Avogadro's number, r_0 the classical electron radius, ρ the mass density, Z the atomic number, and A the molar mass. The radius of the lenses is linear with the number of lenses required and reciprocally linear with the focal length. A line focus is required for an observation of a larger volume, when only a spatial resolution in one direction is needed, such as for studying surfaces, thin films, and interfaces *in situ* and *operando*. It is



also the best choice if the beamline is using a non-source-conserving optic monochromator, such as the single bounce bent-Laue monochromator for polychromatic focusing as used at the high-energy X-ray beamlines 11-ID-B and 11-ID-C at the Advanced Photon Source (APS). Here, the horizontal direction is already moderately focused, and the vertical direction can be focused by CRLs.

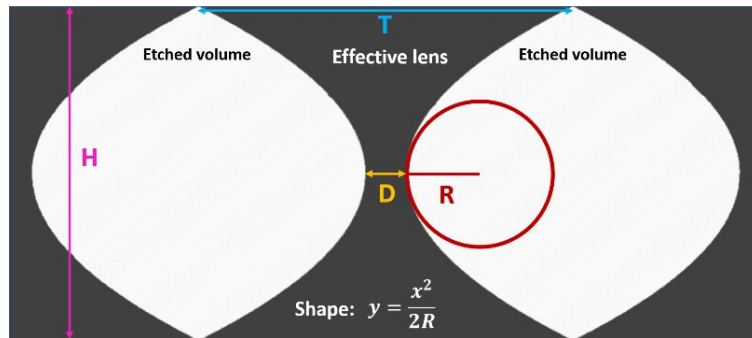


Figure 1: Bi-concave parabolic lenses etched into silicon. H is the height of the lens, T is the width of an individual lens, D the thickness between etched holes. The formula of the shape is included in the figure with x as the vertical direction and y the horizontal.

For 11-ID-B and 11-ID-C, lenses were required to expand the experimental capabilities of these very productive diffraction beamlines with the requirement to change from unfocused to focused beam reliably in a matter of minutes, matching the mission of a high-throughput beamline. The operating photon energies at 11-ID-B are 59 keV and 87 keV with a focal distance of about 1.8 m, and 106 keV at 11-ID-C with a focal distance of about 1.2-1.4 m. Using silicon lenses with a radius of 50 μm , stacks between 80 to 435 lenses are needed under these conditions. Since these beamlines have high experimental throughput, the focusing optics need to be very easy to handle. Therefore, the choice was made to use parabolic shaped lenses etched into silicon which could be fabricated in house for a fraction of the cost. The length of a single lens along the beam is 0.225 mm, so that the physical size of an array of 435 lenses is still less than 100 mm long.

2. Fabrication

The overall fabrication of this type of focusing optics is straightforward and requires only layer of lithography and one deep silicon etch. Lens arrays were patterned via maskless lithography using the Heidelberg MLA 150, with 10-12 μm photoresist. Early devices were fabricated on 4" silicon (Si) wafers, etched in an Oxford Plasmalab 100 ICP-RIE to a depth of $\sim 200 - 400 \mu\text{m}$. Later devices were fabricated on 6" Si wafers, etched in a Plasmatherm Versaline DSE to a depth of $\sim 300 \mu\text{m}$. After etching was completed, individual chips with 3 arrays each were cut using an ADT 7122 dicing saw.

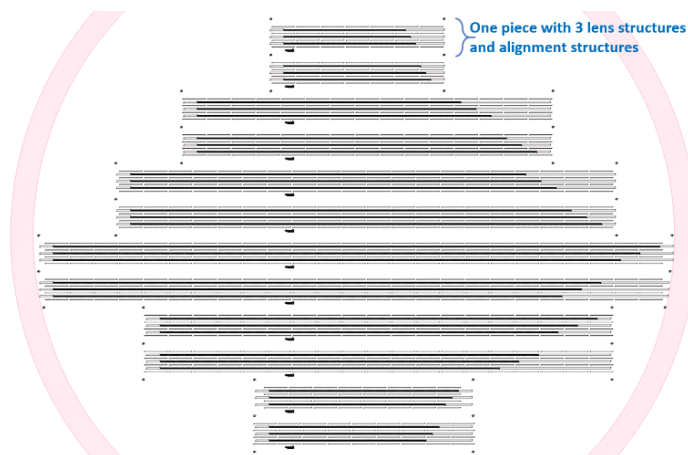


Figure 2: Design of lens arrays on a silicon wafer (red frame) using KLayout [11]. Here, 12 chips with 3 lens arrays each including notches as alignment structures are prepared. After etching, the wafer is diced into chips, which are 8 mm in height and up to 100 mm long. The lens arrays on the chips are 1.5 mm apart from each other.

Our first design using KLayout [11] included parabolic lenses with two radii: $R = 50$ and $R = 65$ μm , in separate lens arrays but on the same wafer. These radii produced lenses of height H between 200 μm and 260 μm with a thickness D of 25 μm , see Figure 1 and 3. Therefore, the width of the single lens is between 225 to 285 μm . The arrays had varying numbers of lenses with the maximum being 490 lenses in one array. Between arrays were notches for alignment in the beam. Prototype wafers were etched to depths between 200 and 400 μm , depending on the success of the etch recipe: maintenance of a reasonable etch rate and survival of the photoresist. Completed wafers were diced into chips, with three lens arrays per chip. Having multiple arrays per chip, with different numbers of lenses per array, allows for quick adjustment of beamline focusing.

Etching deep vertical sidewalls can be a challenge. In general, it is fairly straightforward to tune a Si deep reactive ion etch (DRIE) process to produce a 10:1 ratio, meaning that an etch depth of ~ 250 μm would be reasonably achievable for a ~ 25 μm wide column of remaining Si. Greater ratios can be achieved by further tuning the etch parameters.

SEM images of initial prototype devices, etched in the Oxford Plasmalab 100 ICP-RIE, showed areas of “breakthrough” toward the bottom of the lenses, where the width of the 25 μm column gradually thinned with depth, eventually approaching 0 μm , see Figure 3a. The larger the opening to be etched, the greater this “overetching” effect. Thus, for a more uniform etch, we found it beneficial to choose one R value for lens curvature per wafer. Overetching can also be reduced by tuning the etch parameters to better protect the sidewalls as the etch progresses.

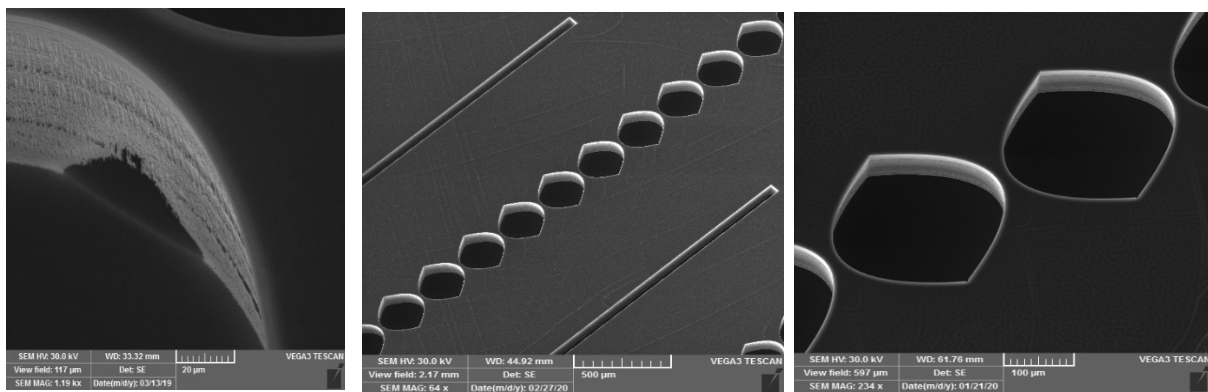


Figure 4: SEM images of the etched structures. On the left is shown the problem of a “breakthrough” of the wall by overetching. This was later better controlled using a new DRIE and optimized parameters as shown in the two pictures on the right.

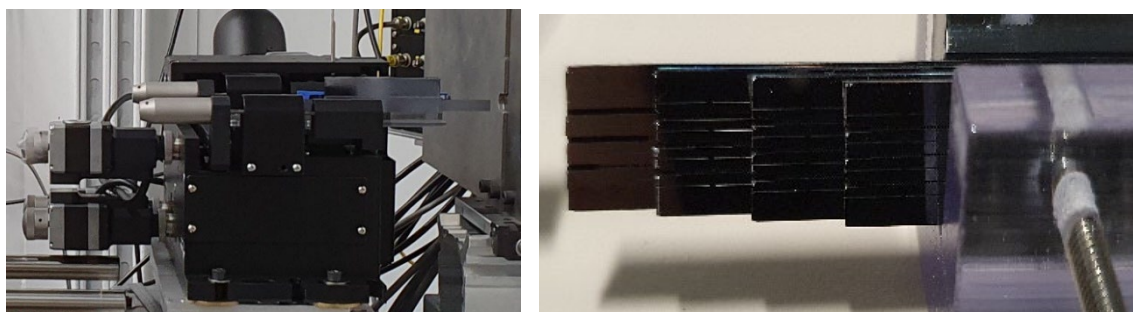


Figure 3: Images of the setup. On the left, the side view of the 6-axes Thorlabs stage is shown. The stack of chips is mounted in the center of rotation. On the right, 4 chips are mounted as a stack giving the options to select 12 different lens arrays to adapt to the photon energy and focal distance.

For later devices, we gained access to a new DRIE tool: a Plasmatherm Versaline DSE. This tool is designed specifically for DRIE and allows for tuning additional etch parameters. After the tool had

been commissioned, etches were quite successful and progressed at a manageable rate ($\sim 2 \mu\text{m}/\text{min}$), without micromasking or overetching, and with minimal wafer heating, see Figure 3.

3. Commissioning at beamlines 11-ID-B and 11-ID-C at APS

11-ID-B and 11-ID-C are side branch beamlines using bent Si-Laue crystals as monochromators under a fixed angle of 7.4° and 4.2° , respectively. The crystals scatter horizontally at the (311) or (422) reflection with asymmetric cut bent to polychromatic focusing condition. The horizontal beam width is approximately 0.4 mm in 11-ID-B and 0.2 mm in 11-ID-C. The lenses are used to focus the beam height, which is unaffected by the monochromator. The distance between source and lenses is about 47 m for 11-ID-B, and the distance to the sample position is between 1.9 m and 2.3 m. For 11-ID-C, the distance between source and lenses is about 52 m with distance to the sample position of 1.5 m.

The stack of chips with lens arrays are mounted on a Thorlab 6-axes positioner for precise alignment, see Figure 4. A translation across the beam moves the stage with the lenses in and out of the beam. Another translation along the beam allows adaptation to the sample-to-lens distance in 11-ID-B.

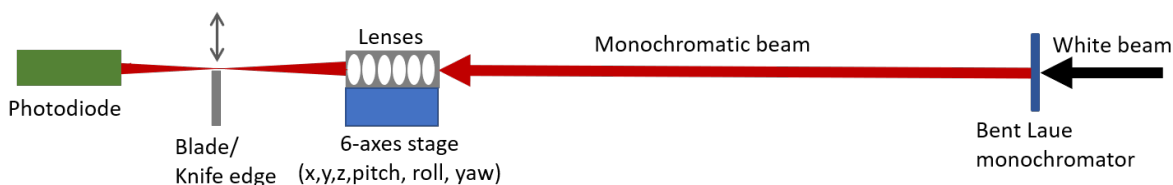


Figure 5: Schematic drawing of the setup to measure the beam profile of the focused beam. The monochromator is about 30 m away from the source. The lens array on the 6-axes stage is 17 m downstream of the monochromator and roughly 1.5 m to 2.3 m before the sample position.

The focused beam was studied by scanning a polished 3 mm thick tungsten blade across the beam, the so-called knife edge scans. The setup is shown in Figure 5. The derivative of the measured intensity behind the blade is the beam profile.

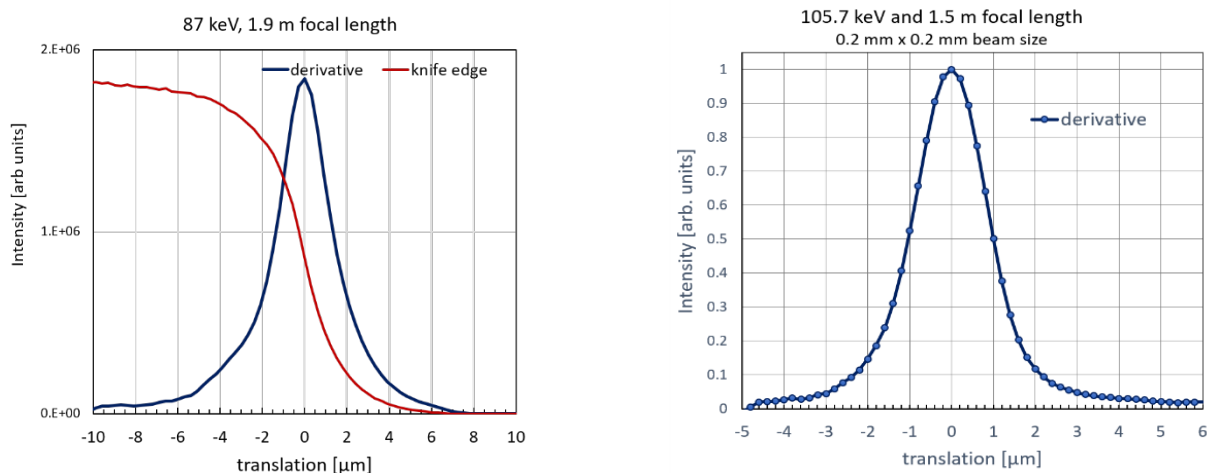


Figure 6: Measured beam profile at focal spot. On the left, the knife edge scan and its derivative are shown for the focus at 11-ID-B using a photon energy of 87 keV and a focal length of 1.9 m. The FWHM is $\sim 4 \mu\text{m}$. On the right, the beam profile at 11-ID-C using 106 keV and a distance of 1.5 m and a lens array of 435 lenses is shown. The measured FWHM is here $\sim 2 \mu\text{m}$.

The smallest focus achieved has a width of $2 \mu\text{m}$, as shown in Figure 6, using a beam size of $0.2 \text{ mm} \times 0.2 \text{ mm}$ before the lens, a photon energy of 105.7 keV and a focal distance of 1.5 m. The lens array had an effective aperture of 0.2 mm. Larger apertures were tested but did not improve the intensity in the focal spot. The acceptance of the horizontal beam size was not limited by the etch depth of the lenses

(300 μm), but rather by the actual beam size which is polychromatically focused by the bent Laue monochromator.

The gain G was determined by comparing the flux density of the unfocused and focused beam. The intensity I_u of the unfocused beam and I_f of the focused beam was normalized with the beam size before the lenses (B_u) and at the focal point (B_f)

$$G = \frac{I_f B_u}{I_u B_f} \quad (2)$$

The intensity ratio was 0.36 and the beam size ratio 100, leading to a gain $G = 36$.

4. Example for application

Whereas the application of total X-ray scattering measurements in transmission geometry and subsequent pair distribution function (PDF) analyses for functional bulk materials is well established, their application to study structure and function of 2-D, interfacial and thin-film materials are presently limited. The main impediment to routine PDF analyses of thin films using the standard approach is the fact that signal generated during transmission geometry measurements is dominated by the contributions from the substrate rather than the sample (film), which consequently hinders reliable and consistent data reduction and PDF extraction. Recently, the possibility of achieving grazing-incidence high-energy total X-ray scattering data of high quality and PDF analyses (GI-PDF) has been demonstrated and suggests opportunities to develop capabilities that are poised to achieve breakthroughs for *in situ* and *operando* structure analyses of functional ultrathin materials. High resolution and surface sensitivity of GI-PDF are needed to suppress background contributions, enabling structural analysis at the atomic scale and quantitative benchmarking to *ab-initio* structure models [12].

This emerging methodology has been recently applied to study the earliest stages of the growth of In_2O_3 ultrathin films via sequential infiltration synthesis (SIS) [13]. A combination of GI-PDF and extended X-ray absorption fine structure was employed to unravel structural evolution of the initially formed $\text{In}_x\text{O}_y\text{H}$ clusters inside a poly(methyl methacrylate) and the formation of In_2O_3 solids upon subsequent SIS cycles. Modelling of the PDF data has revealed that the prime nuclei, formed during the initial SIS stages, exhibits a structure of high ratio (elongated) and evolves into three dimensional network after additional SIS cycles. Annealing the mixed inorganic/polymer films in air removes the PMMA template and consolidates the as-grown clusters into cubic In_2O_3 nanocrystals with structural details that also depend on SIS cycle number.

5. Conclusions

We achieved a focal size of several microns at photon energies above 50 keV with a flux density gain of more than a factor of 30. The efficiency was not improved by choosing larger radii or larger apertures. The radius of 50 μm matched our needs best, and the effective acceptance of the vertical beam is about 200 μm . The lenses have been reliably in use for several years now, and they are set up to be translated into the beam on demand.

The original concept was to create lens arrays such as the ones tested to match the needs of particular beamlines operating at particular energies.

Since the lens arrays can easily be cut, a different approach is to use a layout with long arrays of lenses with identical radii and apertures to optimize the etching process. These arrays can then be cut on demand to provide the optimized number of lenses. This kind of lens arrays in “stock” will optimize the quality of the lenses and increases the flexibility for spontaneously changing demands.

6. Acknowledgement

This research used resources of the Advanced Photon Source and at the Center for Nanoscale Materials, both U.S. Department of Energy (DOE) Office of Science user facilities at Argonne National Laboratory and is based on research supported by the U.S. DOE Office of Science-Basic Energy Sciences, under Contract No. DE-AC02-06CH11357.

References

- [1] A. Snigirev, V. Kohn, I. Snigireva, B. Lengeler 1996 *Nature* **384**, 49-51
- [2] B. Lengeler, J. Tümmler, A. Snigirev, I. Snigireva, and C. Raven 1998 *J. Appl. Phys.* **84** (11), 5855-5861
- [3] <https://www.rxoptics.de/>, April 2022
- [4] S. D. Shastri, J. Almer, C. Ribbing, and B. Cederström 2007 *J. Synchr. Radiat.* **14** (2), 204–211
- [5] <https://www.alcorix.com/product/sawtooth-focusing-devices/>
- [6] V. Aristov, M. Grigoriev, S. Kuznetsov, L. Shabelnikov, V. Yunkin, T. Weitkamp, C. Rau, I. Snigireva, A. Snigirev, M. Hoffmann, and E. Voges 2000 *Appl. Phys. Lett.* **77**, 4058–4060
- [7] F. Stöhr 2015 Microfabrication of hard x-ray lenses. Technical University of Denmark
- [8] C. G. Schroer, M. Kuhlmann, U. T. Hunger, T. F. Günzler, O. Kurapova, S. Feste, F. Frehse, B. Lengeler, M. Drakopoulos, A. Somogyi, A. S. Simionovici, A. Snigirev, I. Snigireva, C. Schug, and W. H. Schröder 2003 *Appl. Phys. Lett.* **82** (9), 1485–1487
- [9] A. Stein, K. Evans-Lutterodt, N. Bozovic, and A. Taylor 2008 *J. of Vac. Sci. & Techn. B: Microelectr. and Nanometer Struct. Process., Meas., and Phen.* **26**, 122-127
- [10] V. Nazmov, E. Reznikova, A. Last, J. Mohr; V. Saile, M. DiMichiel & J. Göttert, 2007 *Nucl. Instr. and Meth. in Phys. Res. A*, 39306, pp. 120-122
- [11] <https://github.com/KLayout/klayout>, April 2022
- [12] A.-C. Dippel, M. Roelsgaard, U. Boettger, T. Schneller, O. Gutowski & U. Ruett 2019 *IUCrJ* **6**, 290-298.
- [13] Xiang He, R.Z. Waldman, D.J. Mandia, N. Jeon, N.J. Zaluzec, O.J. Borkiewicz, U. Ruett, S.B. Darling, A.B.F. Martinson, and D.M. Tiede 2020 *ACS Nano* **14** (11), 14846-14860

The submitted manuscript has been created by UChicago Argonne, LLC, Operator of Argonne National Laboratory (“Argonne”). Argonne, a U.S. Department of Energy Office of Science laboratory, is operated under Contract No. DE-AC02-06CH11357. The U.S. Government retains for itself, and others acting on its behalf, a paid-up nonexclusive, irrevocable worldwide license in said article to reproduce, prepare derivative works, distribute copies to the public, and perform publicly and display publicly, by or on behalf of the Government. The Department of Energy will provide public access to these results of federally sponsored research in accordance with the DOE Public Access Plan. <http://energy.gov/downloads/doe-public-access-plan>